AFRL-ML-WP-TP-2007-403

UNLUBRICATED GROSS SLIP FRETTING WEAR OF METALLIC PLASMA SPRAYED COATINGS FOR Ti6A14V SURFACES (PREPRINT)

Carl H. Hager, Jr., Jeffrey H. Sanders, and Shashi K. Sharma

NOVEMBER 2006

Approved for public release; distribution unlimited.

STINFO COPY

MATERIALS AND MANUFACTURING DIRECTORATE
AIR FORCE RESEARCH LABORATORY
AIR FORCE MATERIEL COMMAND
WRIGHT-PATTERSON AIR FORCE BASE, OH 45433-7750

NOTICE AND SIGNATURE PAGE

Using Government drawings, specifications, or other data included in this document for any purpose other than Government procurement does not in any way obligate the U.S. Government. The fact that the Government formulated or supplied the drawings, specifications, or other data does not license the holder or any other person or corporation; or convey any rights or permission to manufacture, use, or sell any patented invention that may relate to them.

This report was cleared for public release by the Air Force Research Laboratory Wright Site (AFRL/WS) Public Affairs Office and is available to the general public, including foreign nationals. Copies may be obtained from the Defense Technical Information Center (DTIC) (http://www.dtic.mil).

AFRL-ML-WP-TP-2007-403 HAS BEEN REVIEWED AND IS APPROVED FOR PUBLICATION IN ACCORDANCE WITH ASSIGNED DISTRIBUTION STATEMENT.

*//Signature//

JEFFREY H. SANDERS, Chief
Nonstructural Materials Branch
Nonmetallic Materials Division

//Signature//

SHASHI K. SHARMA, Acting Deputy Chief
Nonmetallic Materials Division
Materials and Manufacturing Directorate

This report is published in the interest of scientific and technical information exchange, and its publication does not constitute the Government's approval or disapproval of its ideas or findings.

*Disseminated copies will show "//Signature//" stamped or typed above the signature blocks.

REPORT DOCUMENTATION PAGE

Form Approved
OMB No. 0704-0188

1. REPORT DATE ***(DD-MM-YY)***
November 2006

2. REPORT TYPE
Journal Article Preprint

3. DATES COVERED ***(From - To)***

4. TITLE AND SUBTITLE
UNLUBRICATED GROSS SLIP FRETTING WEAR OF METALLIC PLASMA SPRAYED COATINGS FOR Ti6A14V SURFACES (PREPRINT)

5a. CONTRACT NUMBER
F33615-03-D-5801

5b. GRANT NUMBER

5c. PROGRAM ELEMENT NUMBER
62102F

6. AUTHOR(S)
Carl H. Hager, Jr. (Universal Technology Corporation)
Jeffrey H. Sanders and Shashi K. Sharma (AFRL/MLBT)

5d. PROJECT NUMBER
4349

5e. TASK NUMBER
LO

5f. WORK UNIT NUMBER
VT

7. PERFORMING ORGANIZATION NAME(S) AND ADDRESS(ES)

Universal Technology Corporation
1270 N. Fairfield Road
Dayton, OH 45432

Nonstructural Materials Branch (AFRL/MLBT)
Nonmetallic Materials Division
Materials and Manufacturing Directorate
Air Force Research Laboratory, Air Force Materiel Command
Wright-Patterson Air Force Base, OH 45433-7750

8. PERFORMING ORGANIZATION REPORT NUMBER

9. SPONSORING/MONITORING AGENCY NAME(S) AND ADDRESS(ES)
Materials and Manufacturing Directorate
Air Force Research Laboratory
Air Force Materiel Command
Wright-Patterson AFB, OH 45433-7750

10. SPONSORING/MONITORING AGENCY ACRONYM(S)
AFRL-ML-WP

11. SPONSORING/MONITORING AGENCY REPORT NUMBER(S)
AFRL-ML-WP-TP-2007-403

12. DISTRIBUTION/AVAILABILITY STATEMENT
Approved for public release; distribution unlimited.

13. SUPPLEMENTARY NOTES
Journal article submitted to WEAR Magazine.
The U.S. Government is joint author of this work and has the right to use, modify, reproduce, release, perform, display, or disclose the work.
PAO Case Number: AFRL/WS 06-2787, 04 Dec 2006.

14. ABSTRACT
Plasma sprayed Al-bronze (Al-Br) or CuNiIn coatings are often applied to protect against fretting wear and extend the operational life of Ti-alloy compressor blades in turbine engines. In order to develop a fundamental understanding of how these coating systems perform under gross slip fretting conditions, bench level fretting wear tests were conducted at room temperature to simulate cold engine startup. Alternative coatings such as plasma sprayed molybdenum and nickel were also evaluated because of their potential for reducing fretting wear under certain simulated engine conditions. The combination of scanning electron microscopy (SEM), surface profilometry, surface chemistry (EDS), and friction analysis were used to study coating performance and evaluate the interfacial wear mechanisms. In this study it was determined that all coatings caused significant damage to the mating Ti6A14V surfaces.

15. SUBJECT TERMS
Fretting wear, Ti6A14V, gross slip, coatings

16. SECURITY CLASSIFICATION OF: a. REPORT	b. ABSTRACT	c. THIS PAGE	17. LIMITATION OF ABSTRACT:	18. NUMBER OF PAGES	19a. NAME OF RESPONSIBLE PERSON (Monitor)
Unclassified	Unclassified	Unclassified	SAR	40	Jeffrey H. Sanders

19b. TELEPHONE NUMBER *(Include Area Code)*
N/A

Standard Form 298 (Rev. 8-98)
Prescribed by ANSI Std. Z39-18

Unlubricated Gross Slip Fretting Wear of Metallic Plasma Sprayed Coatings for Ti6Al4V Surfaces

C.H. Hager, Jr. (Contact Author)
Universal Technology Corporation
1270 North Fairfield Road
Dayton, OH 45432-2600
(937) 255-9016
carl.hager@wpafb.af.mil

J.H. Sanders and S. Sharma
2941 Hobson Way AFRL/MLBT
Wright Patterson Air Force Base, OH 45433-7750

Abstract

Plasma sprayed Al-bronze (Al-Br) or CuNiIn coatings are often applied to protect against fretting wear and extend the operational life of Ti-alloy compressor blades in turbine engines. In order to develop a fundamental understanding of how these coating systems perform under gross slip fretting conditions, bench level fretting wear tests were conducted at room temperature to simulate cold engine startup. Alternative coatings such as plasma sprayed molybdenum and nickel were also evaluated because of their potential for reducing fretting wear under certain simulated engine conditions. The combination of scanning electron microscopy (SEM), surface profilometry, surface chemistry (EDS), and friction analysis were used to study coating performance and evaluate the interfacial wear mechanisms. In this study it was determined that all coatings caused significant damage to the mating Ti6Al4V surfaces.

Key Words

Fretting Wear, Ti6Al4V, Gross Slip, Coatings

1. Introduction

Fretting wear is an accumulation of damage that occurs at component interfaces that are subjected to high contact stresses coupled with low amplitude oscillation. This phenomenon often leads to the immediate disruption of surface oxides within the contact. Depending on the chemistry and morphology of the oxide debris, these particles can cause abrasive wear between the contacting surfaces. Once the surface oxides have been removed, the nascent surfaces are exposed and typically adhere causing adhesive wear, or galling in some cases, to occur until the wear particles are broken up into finer debris and eventually oxidized [1]. Evidence of this for Ti6Al4V mating surfaces has been noted in this study in the wear mode analysis section.

In the aerospace industry fretting wear can be problematic, often leading to catastrophic failures. One of the most common occurrences of fretting in a jet turbine engine is in the compressor section at the blade/disk interface. The blade/disk interface, also known as the dovetail joint, is often fabricated from Ti6Al4V because of its high strength to weight ratio and corrosion resistance. Tribologically, mating Ti6Al4V surfaces are especially susceptible to fretting because titanium alloys have a propensity to gall and can produce hard oxide debris that score the interface [2-4]. In addition to fretting wear at the interface, the combination of the rotating disk and the airflow through the engine imposes centrifugal forces and radial oscillations on the blades causing bulk cyclic stresses and component fatigue. The combination of the bulk cyclic stresses and fretting surface interactions is often called fretting fatigue [5-7]. The impact of fretting wear on the reduction of fatigue life has been addressed in many publications. However, Zhou et al. conducted a study using aluminum alloys that showed fretting wear can cause surface tears or cracks that are long enough to be considered critical without bulk loading to the specimen [8]. This study demonstrates how detrimental fretting wear can be to the fatigue life of contacting specimens, even when they are not in the presence of fatigue loading.

A common solution to the fretting wear/fatigue problem is to apply plasma sprayed coatings and solid lubricants to the component surfaces [8-10]. Although the implementation of coatings and lubricants has increased component life, there is a tremendous cost associated with schedule based maintenance of these systems. Therefore, the development of new coatings, coating processes, and lubricants that are able to reduce fretting damage and withstand the hostile engine environment will provide significant reductions in maintenance costs. In order to develop these coatings, it is important to characterize the Ti6Al4V surface interactions with current coatings and compare them with potential replacement materials. In this study, an in depth evaluation was conducted on the gross slip fretting wear of Ti6Al4V mated surfaces as well as Ti6Al4V worn against plasma sprayed copper-nickel-indium (CuNiIn), aluminum-bronze (Al-Br), molybdenum (Mo), and nickel (Ni). CuNiIn and Al-Br are the two most prominent thermal sprayed coatings for this application, while the Mo and Ni coatings are two wear resistant coatings that have some potential for fretting wear mitigation [9, 11, and 12]. Fretting experiments and post test analysis were used to determine the performance of these unlubricated coating systems at room temperature.

2. Experimental

2.1 Specimens

The specimens used for this investigation were Ti6Al4V, and the test geometry was an ellipsoid on a flat plate. The ellipsoid, shown in Fig. 1, was designed to eliminate the stress concentrations that occur at the edges of cylindrical contacts. Therefore, the Hertzian contact stress profiles for the samples are smooth with a maximum stress at the center instead of near the edge of contact. In addition, the elliptical contact simplifies alignment procedures for reproducible contact areas, and the large radius in the sliding direction allows for a target maximum Hertzian contact pressure of 650 MPa with an applied normal load of 50 N. The plates were flat circular disks with a diameter of 12.7 mm on the test face and 3.2 mm thick. Average surface roughness (Ra) was 0.1μm on both the disk and ellipsoid. Prior to testing, the Ti6Al4V disks were commercially grit blasted and then plasma sprayed with CuNiIn, Al-Br, Mo, and Ni. The coatings were all in the range of approximately 75-100μm thick. The coating compositions, surface roughness, hardness, and modulus measurements are listed in Table 1. Metallography of coatings showed that the Al-Br coatings were less uniform and less dense than the other coatings, which is reflected in the measured hardness values.

2.2 Tribological Testing and Analysis

The purpose of this study was to provide an understanding of how Ti6Al4V performed when coupled with the selected metallic plasma sprayed coatings, and subjected to gross slip fretting wear at room temperature. The room temperature tests were designed to simulate cold engine startup. Three to four repeat tests were conducted on each coating. The tests were conducted using a 200μm stroke length, 30Hz oscillation speed, and a 50N normal load for 100,000 cycles. The applied 50N normal load yields a maximum Hertzian contact stress of approximately 650MPa. In addition, shorter duration tests were conducted at 2 Hz oscillation speed, to supplement the longer tests for wear analysis.

For the duration of each test the root mean square (RMS) of the friction data and the frictional hysteresis was recorded. The fretting wear tribometer, illustrated in Fig 2, has a stage that is mounted on thin metal legs that can support the normal applied load, while acting as tangential springs in the oscillation direction. As the elliptical sample moves the friction force between the samples causes the sample stage to deflect slightly, on the order of 1 μm typically, in the direction of sliding. The stage deflection then compresses or stretches the attached piezoelectric transducer and creates a signal. The signal from the piezo is then amplified and calibrated, using a force meter, to match the amount of force applied to the stage prior to testing. The friction force is then collected using an oscilloscope data acquisition card and a computer. Once collected, the RMS of the friction force is then tabulated and plotted per test cycle in situ. In addition, a laser measuring system, shown in Fig 2, is focused on the face of the oscillating arm of the tribometer and is used to continuously track the displacement of the ellipsoid during each test. The real time displacement data along with friction data and are then collected using the same oscilloscope computer card and are plotted to produce in situ hysteresis loops that provide real time monitoring of the fretting wear regime.

There have been a number of papers published that explain the use of hysteresis loops for the determination of fretting wear regime [14-20]. Elliptical shaped hysteresis loops have been shown to depict mixed fretting behavior and quasi-rectangular shaped hysteresis loops have been shown to depict gross slip behavior. This technique was used to ensure that each test operated in the gross slip regime throughout the entire duration of the test.

Once the fretting wear tests were completed, post test analysis was performed using scanning electron microscopy (SEM) and 3-D contact profilometery for morphology, along with energy dispersive spectroscopy (EDS) for chemical analysis. All cross-sections were cut perpendicular to the fretting wear direction using a low speed diamond saw. The coating cross-sections were mounted using an air cured epoxy mount, and the uncoated ellipses were mounted using a hard carbon filled conductive hot compression mount. The hot compression mounts were used on the ellipse cross-sections because they have a higher hardness and better edge retention, which is needed to keep the worn regions intact during the polishing process. Once mounted, all cross-sectioned samples were polished prior to microstructure and EDS analysis.

3 Results

3.1 Friction and Wear

The coefficients of friction for all the tests ranged from approximately 0.7 to 0.9. Fig 3 shows typical friction traces measured during the course of the fretting tests, and shows that the addition of the coatings to the interface does not significantly reduce the friction. Only the CuNiIn coating reduced the measured friction coefficient from the 0.8 exhibited by Ti6Al4V mating surfaces down to 0.7.

In addition to measuring the friction, the coating wear was assessed by determining the maximum depth in each wear track using a 3-D contact profilometer. Fig 4 shows the average depths measured for each configuration tested. The Mo coating was the hardest and most wear resistant of all the coatings at room temperature, while

CuNiIn exhibited the most wear. However, none of the coatings wore completely through to the substrate.

3.2 Wear Mode Analysis

This study consisted of fretting wear tests in which Ti6Al4V ellipsoids were worn against Ti6Al4V, CuNiIn, Al-Br, Mo, and Ni. In addition to the 30 Hz and 100,000 cycle tests at room temperature, short duration tests conducted at 2 Hz oscillation speed were conducted for further insight. Uncoated Ti6Al4V specimens were tested as a baseline to quantify how well the coatings protect the mating Ti6Al4V surfaces. Specifically, the ellipsoid wear in the uncoated case will be used as a comparison to assess the amount of damage on the ellipsoids caused by fretting against the coated surfaces. In this section the wear on the coatings as well as in the uncoated contacts will be discussed.

3.2.1 Uncoated Ellipsoid Wear

At room temperature the Ti6Al4V mating surfaces are damaged primarily by galling initially, and then by 3rd body wear as the large adhered particles start to break apart. After 10 cycles, with 2 Hz oscillation speed, the gross slip fretting wear at the Ti6Al4V interface of the test specimens is composed of solely adhesive wear, as shown in Fig 5A. The mated surfaces exhibited severe plastic deformation with large wear particles, on the order of 100 µm long and 50 µm wide, adhered to the wear track. After 100 cycles the large wear particles in the contact start to break up into smaller wear debris, as shown in Fig 5B. The majority of the debris gathers around the edges of the contact, with some of the debris getting trapped inside the wear track. After 1,000 cycles almost the entire wear track is filled with wear debris, as shown in Fig 5C. Some large wear particles can be seen near the center and the edges of the wear track. Some of these larger particles are produced in local regions throughout the wear track where the Ti6Al4V surfaces make contact in the absence of the trapped wear debris, and some of the particles are from the adhesive wear that was predominant during the initial stages of the test. After 100,000 cycles, with 30 Hz oscillation speed, the wear track is completely filled with wear debris, as shown in Fig 5D. This exact wear mode has been described in detail in a fretting wear review paper by Hurricks [1], and by Blau [21] in his work with wear mechanisms in metallic interfaces. Fig 6A and 6B shows cross-sectional micrographs of a typical 100,000 cycle Ti6Al4V mating fretting wear test. The cross-sections of the ellipsoid wear tracks were cut perpendicular to the fretting direction as shown by the arrows in Fig 5D. In the center of the wear track, the wear scar is approximately 30 to 40 µm deep. The dark region shows a compacted powder bed of fine titanium and oxide wear debris. Using Raman Spectroscopy, Hager et al [13] determined that the accumulation of gross slip fretting wear debris in the contact of Ti6Al4V mating surfaces contains significant amounts of rutile TiO_2. Fig 6B shows the plastically deformed surface layers, or highly deformed layer (HDL) as defined by Rigney et al [22], near the edge of the wear scar and beneath the trapped wear debris. In these contact regions the accumulation of plastic deformation occurs until the surface material becomes too brittle to accommodate the imposed strain, as explained by Blanchard et al [23]. This eventually leads to the breakup of surface regions and the formation of large wear particles, as shown in Fig 6B.

The wear mode analysis conducted on the uncoated Ti6Al4V ellipsoids, worn against the plasma sprayed CuNiIn, Al-Br, Mo, and Ni coatings, determined that the wear evolution and damage mechanisms are same as those exhibited by mated Ti6Al4V surfaces. Figs 7 shows SEM micrographs of the ellipsoid surface damage caused by gross slip fretting against each of the plasma sprayed coatings. After just 100 cycles, the accumulated damage is driven by adhesive wear. EDS analysis and X-ray mapping of the magnified regions showed that the large adhered particles, in all four wear tracks, are adhered metallic particles from the various coating surfaces. These large adhered particles plow large channels or make striations on the surface of the Ti6Al4V ellipsoids. In addition, the micrographs from these tests also show a significant amount of tiny wear debris trapped within the wear track. Using EDS, it was determined that these particles are a mixture of mostly oxidized Ti6Al4V and transferred coating wear debris.

Although the apparent mechanisms by which the fretting wear has damaged the surface of the Ti6Al4V ellipsoids are the same against all of the coated and uncoated surfaces, the accumulation and evolution of the wear at each interface still exhibited some distinct characteristics. All of the worn Ti6Al4V ellipsoid surfaces had adhered coating particles. However, these particles varied in size and in the amount of damage they caused. Wear against the CuNiIn coating for 100 cycles produced large adhered coating particles, on the order of 20 to 100μm in size. In addition, 100 cycles of fretting was enough to cause galling throughout most of the contact area and create large amounts of trapped oxide debris, the tiny white particles that are dispersed throughout the wear track as shown in Fig 7A. Fretting for 100 cycles against the Al-Br coating caused the least amount of damage to the Ti6Al4V ellipsoid, in comparison to all of the coatings tested. Fig 7B shows that the Al-Br coating smeared onto the Ti6Al4V surface causing galling to occur only in localized regions. The Mo coating, which was the hardest of the four coatings, caused the most severe damage to the mated Ti6Al4V surface, after 100 cycles.

Adhesion between the coating and the Ti6Al4V ellipse caused severe galling and the transfer of large Mo particles. The adhered Mo particles, typically on the order of 100 μm in size, mixed with the displaced titanium at the edges of the galled regions, as shown in Fig 7C. Fretting against the Ni coating for 100 cycles produced a wear track on the Ti6Al4V mated ellipsoid that was similar to what was seen in the CuNiIn tests. The differences between the two are that the Ni created a wear scar with deeper galling tracks and more fine oxide debris trapped within the contact, as shown in Fig 7D.

Figs 8 shows micrographs of the ellipsoid wear after 1,000 and 100,000 cycle tests. In the 1,000 cycle tests conducted against Mo and Ni, Fig 8E and 8G respectively, the micrographs show that the gross slip fretting wear progression of the interfaces has lead to the break up and oxidation of the large galling products and the protruding Ti6Al4V at the edges of the severely deformed regions that were seen in the 100 cycle tests. Therefore, the interfacial wear on the ellipsoid has transitioned from adhesive wear and galling to a 3rd body abrasive wear during the period between 100 and 1,000 cycles. In the 1,000 cycle tests conducted against CuNiIn and Al-Br, Fig 8A and 8C respectively, the wear tracks show an increased amount of fine oxide debris trapped within the wear track, and the absence of the large transfer particles that were seen in the 100 cycle tests. However, the wear scars created by CuNiIn and Al-Br exhibited large regions near the center of the contact where evidence of adhesive wear was still apparent. After 100,000 wear cycles all surfaces of the wear tracks against each of the different coatings were completely covered with a powder bed of compacted wear debris. This debris was composed of mostly oxidized Ti6Al4V and coating particles along with some larger metallic particles, typically from the coating surfaces. Micrographs of the ellipsoid wear tracks after 100,000 cycles are shown in Fig 8.

In addition to the wear scar surface analysis, all of the Ti6Al4V ellipsoids worn for 100,000 cycles were cross-sectioned perpendicular to the fretting direction, shown by the black arrows in Fig 5D, 8B, 8D, 8F, and 8H. Analysis of the back scatter (BSE) SEM micrographs of the ellipsoid cross-sections, shown in Fig 9, further verifies the similarities in the fretting wear mechanisms that damage these Ti6Al4V surfaces when self mated or worn against the CuNiIn, Al-Br, Mo, or Ni plasma sprayed coatings. Fretting wear of Ti6Al4V ellipsoid surfaces mated with the CuNiIn and Al-Br coatings produced virtually identical wear to that of the mating Ti6Al4V surfaces, as seen by comparing Figs 9A-9D with Figs 5A and 5B. The only differences being that the mixture metal and oxide debris compacted into the worn ellipsoid surfaces have different chemistries, and that the ellipsoids worn against Al-Br did not have the large detached particles that were seen in the CuNiIn tests, as shown in comparing Fig 9B and 9D. The wear scars from fretting against CuNiIn and Al-Br have compacted debris composed of oxidized debris from the coating surfaces mixed with the titanium and titanium oxide debris, as confirmed with EDS analysis. The wear on the ellipsoid surfaces mated with the Mo and Ni coatings, shown in Figs 9E and 9F, also exhibit similar wear mechanisms. However, these surfaces have thinner transfer films of compacted debris and larger Ti6Al4V wear particles. Often these Ti6Al4V particles are on the order of 50μm deep and just as wide. This is typically 2 to 3 times larger than the ones seen at the CuNiIn worn Ti6Al4V interfaces.

3.2.2 Coating Wear

After 100 fretting wear cycles at 2 Hz, the wear on the surface of the coatings was localized to the damage of the large asperity tips of the rough as sprayed coatings. Fig 10 shows secondary electron and back scatter (BSE) SEM images of the wear tracks. In both sets of images it can be seen that the surface asperities of the CuNiIn, Al-Br, and the Ni coatings have been sheared and flattened, with the produced debris collected in the valleys of the coating surface. Unlike the other three coatings, the Mo coating sustained almost no surface damage after 100 cycles. However, the surface of the Mo coating did have debris trapped in the valleys between the asperities as seen on the other coatings. The BSE images, shown in Fig 10, display changes in contrast with respect to changes in surface chemistry. Therefore the dark regions that are shown with arrows in Fig 10A, 10C, and 10D indicate Ti6Al4V particles that have adhered to the coating surface. This fact was further verified chemically using EDS. The Al-Br coating, shown in Fig 10B, was the only one of the tested coatings that did not have large pieces of the mated Ti6Al4V ellipsoid surface adhered to the coating wear track.

Extended fretting wear tests lead to the continued shearing of large coating asperities, as well as the breakup of the transferred Ti6Al4V particles that were seen after 100 cycles of wear. Fig 11 shows SEM images of the coating wear tracks after 1,000 and 100,000 cycle tests. The separate sets of tests were conducted respectively at 2 Hz and 30 Hz oscillation speeds. After 1,000 cycles, the coating asperities have been worn away completely, except on the Mo coating. The wear debris that was once trapped in the valleys between asperities is swept towards the edges of the wear track, leaving enough debris trapped within the contact to cover a large portion of the contact region. The Al-Br coating, Fig 11C, is the only coating with significant surface area that is uncovered by wear debris within the wear track after 1,000 cycles. After 100,000 cycles the wear tracks of coatings appeared to have reached steady state wear. With the exception of the Mo coating, the wear tracks were significantly covered with debris creating a powder bed within the contact, as shown in Fig 12. This indicates that the interfacial wear mechanisms are now controlled by the rheology of the wear debris trapped within the contact, as studied by Colombie et al [24], as well as by any localized metallic contact that may occur. However, the Mo coating, even after 100,000 cycles, still has valleys between the asperities that trap debris. In addition, there are some localized regions in the Mo wear tracks where EDS showed a concentration of titanium material. Fig 13 and Fig 14 show average ratios of the Ti/coating and oxygen/Ti in atomic % as measured using EDS. These measurements were made in the dark regions of the BSE SEM images, as seen in Fig 12. In the localized dark regions, the Mo has a Ti/Mo ratio of more than 1.5/1 and an oxygen/Ti ratio of approximately 3/1. Molybdenum will oxidize typically to MoO_3 and titanium will oxidize typically to TiO_2; therefore, there is not enough oxygen detected in these regions for the debris to be completely oxidized. This indicates that even after 100,000 cycles the Mo coating is still galling in localized regions.

4. Summary and Discussion

In overview, this study was conducted to assess the interfacial wear mechanisms associated with gross slip fretting of Ti6Al4V in contact with four different thermal spray coatings at room temperature. These tests were conducted without lubrication and caused metallic wear in the fretting contact. All metallic engineering surfaces are covered by thin oxide layers that are typically angstroms or nanometers in thickness [1, 25]. This contaminant layer initially protects the underlying metal. However, surface species are dispersed during the first few cycles of the fretting wear process causing the intimate contact of the Ti6Al4V ellipsoid surfaces with the metallic coating surfaces. When this happens the contacting nascent metallic surfaces cause adhesive wear and ultimately galling. The galling of the Ti6Al4V ellipsoid surface coincides with the shearing of the coating surface asperities, and the simultaneous transfer metallic material between the contacting surfaces.

All of the coatings tested were approximately half as hard as the Ti6Al4V contact surface, with the exception of the Mo coating which was slightly harder than its titanium counterpart. This would lead one to believe that material transfer at the fretting interface would consist of the softer coating surfaces transferring to the harder Ti6Al4V surface, and in fact this is what predominantly occurs. However, there are localized regions where large Ti6Al4V particles, on the order of 50 to 100μm, were adhered to the surfaces of the CuNiIn and Ni coating surfaces. Bowden et al [26] also witnessed a similar phenomenon when they observed the transfer of small fragments of mild steel to the surface of copper during sliding wear experiments. This is an extremely devastating wear phenomenon that accelerates the ellipsoid wear, because the Ti6Al4V adhered particles form raised plateaus on the coating surface and promote further galling by creating titanium on titanium contact within the fretting interface.

Galling and material transfer, along with the shearing of coating asperities typically occurs within the first 100 gross slip fretting wear cycles. Between 100 and 1,000 cycles of wear, the highly deformed surface layer of the Ti6Al4V ellipsoid becomes too brittle to accommodate the imposed fretting displacement, as explained by

Blanchard et al [23], and begins to crack and break, as shown in Fig 6B. In addition, the continued deformation of the transferred material plateaus causes them to breakup as well. This creates an abundance of wear debris within the contact. The wear debris represents a wear mode shift from adhesive driven wear to wear that is mostly driven by the rheology of the 3rd body debris, most likely 3rd body abrasion.

From 1,000 cycles to 100,000 cycles some of the wear debris is swept out of the wear track, and some of the wear debris remains. The trapped or active wear debris continuously gets crushed into fine particles and oxidizes. As the active wear debris builds up in the wear track, it gets compressed together and forms a powder bed that separates the contacting surfaces. If the powder bed formation is continuous, as it is in the cross sections of the ellipsoids worn against CuNiIn and Al-Br shown in Fig 9A and 9C, then the surface degradation will be concentrated at the edges of the contact and expand the wear track laterally instead of deeper. This can be seen in Fig 9B and 9D. In the case of the Mo coating, the asperities are never completely worn away and the valleys trap the wear debris preventing the formation of a powder bed. This is why there is still evidence of localized galling near the center of the wear track after 100,000 fretting wear cycles.

Ultimately, the thermal spray coatings tested did not change the associated wear mechanisms or reduce the apparent wear damage imposed on the Ti6Al4V ellipsoid surface. Although the wear may have appeared to be reduced in the first 100 cycles or so against the Al-Br coating, the eventual result after 100,000 cycles of gross slip fretting wear was the same as that seen in the Ti6Al4V mating contacts. This is because of the formation of a powder bed in all of the tested configurations. The rheology of the 3rd

body debris, primarily the titanium oxide debris which is constant to all of the tests, controls the extent of the fretting wear damage to the Ti6Al4V ellipsoid after 1,000 cycles, or once enough debris has been established in the contact. In addition, the CuNiIn, Al-Br, and Ni thermal spray coatings sustained severe wear during each of the fretting wear tests. 30% to 40% of the coating thickness had been worn away after 100,000 cycles of fretting. The Mo coatings were very wear resistant and exhibited wear scars that were half the depth of the other coatings. However, the wear resistance of the Mo coatings can be more detrimental to the Ti6Al4V ellipsoid due to the localized galling that continues for at least two orders of magnitude longer than against the other coatings tested.

The wear analysis from this study supports the need for a different coating system than the current rationale. Although the actual compressor blades are coated with thermal sprayed coatings and then with solid lubricants, this study shows the dangers of what can happen if/or when the lubricants fail or are completely worn away. In gross slip fretting, these soft thermal spray coatings do not effectively protect the mating Ti6Al4V surfaces without solid lubrication.

5. Conclusions

This study was conducted to examine the wear mechanisms associated with the addition of four thermal sprayed coatings into a Ti6Al4V mated fretting contact, under gross slip. It was found that:

- The measured coefficient of friction in all of the tests was very high, from 0.7 to 0.9.

- All of the wear mechanisms that governed the surface damage accumulation were the same in all of the tested coating configurations.
- All of the extended tests exhibited similar amounts of Ti6Al4V ellipsoid wear against all of the coatings and in the Ti6Al4V mated tests. Therefore, all of the coatings tested were unable to adequately protect the mated ellipsoids without lubrication.

Reference:

[1] P. Hurricks, The mechanisms of fretting – a review, *Wear* 15 (1970) 389-409.

[2] S. Fayeulle, P. Blanchard, L. Vincent, Fretting behavior of titanium alloys, *Tribology Transactions* 36 (1993) 267-275.

[3] E. Sauger, S. Fouvry, L. Ponsonnet, P. Kapsa, J. Martin, L. Vincent, Tribologically transformed structure in fretting, *Wear* 245 (2000) 39-52.

[4] M. Long, H. Rack, Friction and surface behavior of selected titanium alloys during reciprocating sliding motion, *Wear*, 249 (2001) 158-168.

[5] R. Waterhouse, Fretting fatigue, *International Materials Reviews*, 37 (1992) 77-97.

[6] T. Lindley, Fretting fatigue in engineering alloys, *International journal of fatigue*, 19 (1997) 39-49.

[7] D. Hoeppner, Mechanisms of fretting fatigue and their impact on test methods development, *ASTM*, STP 1159 (1992) 23-32.

[8] Z. R. Zhou, L. Vincent, Mixed fretting regime, *Wear* 181-183 (1995) 531-536.

[9] J. DeMasi-Marcin, D. Gupta, Protective coatings in the gas turbine engine, *Surface and Coatings Technology* 68-69 (1994) 1-9.

[10] A. Freimanis, A. Segall, J. Conway Jr., E. Whittney, The influence of temperature and wear mode on the deterioration of coatings used for titanium aircraft engine components, *Tribology Transactions* 45 (2002) 193-198.

[11] H. Privett III, S. Fujishiro, Coating studies for prevention of fretting fatigue in jet engine titanium compressor blade dovetails, *Metallurgy and technology of practical titanium alloys*, (1994) 401-410.

[12] S. Harris, M. Overs, and A. Gould, “The use of coatings to control fretting wear at ambient and elevated temperatures,” *Wear*, 106 (1985) 35-52.

[13] J. Okado, M. Shima, I. McColl, R. Waterhouse, T. Hasegawa, M. Kasaya, “Ni-P and Mo: an excellent fretting wear resistant combination,” *Wear*, 225-229 (1999) 749-757.

[14] C. Hager, Jr., J. Sanders, and S. Sharma, “Characterization of Mixed and Gross Slip Fretting Wear Regimes in Ti6Al4V Interfaces at Room Temperature,” *Wear*, 257 (2004) 167-180.

[15] H. Deresiewicz, R. D. Mindlin and applied mechanics, Pergamon Press Inc., New York, 1974.

[16] S. Fouvry, P. Kapsa, H. Zahouani, L. Vincent, Wear analysis in fretting of hard coatings through dissipated energy concept, *Wear* 203-204 (1997) 393-403.

[17] O. Vingsbo, J. Shön, Gross slip criteria in fretting, *Wear* 162-164 (1993) 347-356.

[18] O. Vingsbo, S. Söderberg, On fretting maps, *Wear* 126 (1988) 131-147

[19] A. Ramalho, J. Celis, Fretting laboratory tests: Analysis of the mechanical response of test rigs, *Tribology Letters* 14 (2003) 187-196.

[20] S. Fouvry, P. Kapsa, L. Vincent, Analysis of sliding behavior for fretting loadings: determination of transition criteria, *Wear* 185 (1995) 35.

[21] P. Blau, Mechanisms for transitional friction and wear behavior of sliding metals, *Wear* 72 (1981) 55-66.

[22] D. Rigney, J. Hirth, Plastic deformation and sliding friction of metals, *Wear* 53 (1979) 345-370.

[23] P. Blanchard, C. Colombie, V. Pellerin, S. Fayayeulle, L. Vincent, Material effects in fretting wear: Application to iron, titanium, and aluminum alloys, *Metallurgical Transactions* 22A (1991) 1535-1544.

[24] C. Colombie, Y. Berthier, A. Floquet, L. Vincent, Fretting: Load Carrying Capacity of Wear Debris, *Transactions of the ASME* 106 (1984) 194-201.

[25] N. Tomashov, *Theory of Corrosion and Protection of Metals*, Macmillan, London, 1966.

[26] F. Bowden, A. Moore, D. Tabor, The ploughing and adhesion of sliding metals, *Journal of Applied Physics* 14 (1943) 80-91.

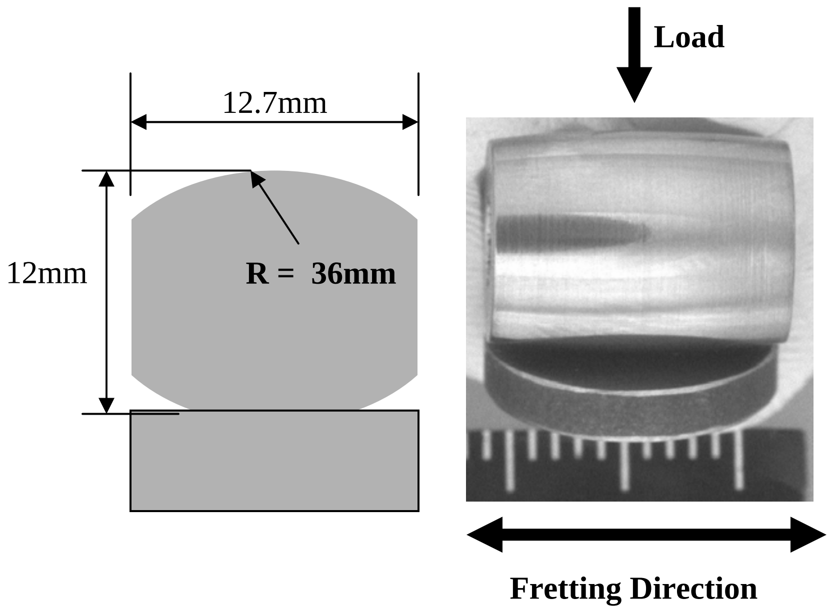

Fig. 1. Ellipsoid contact geometry.

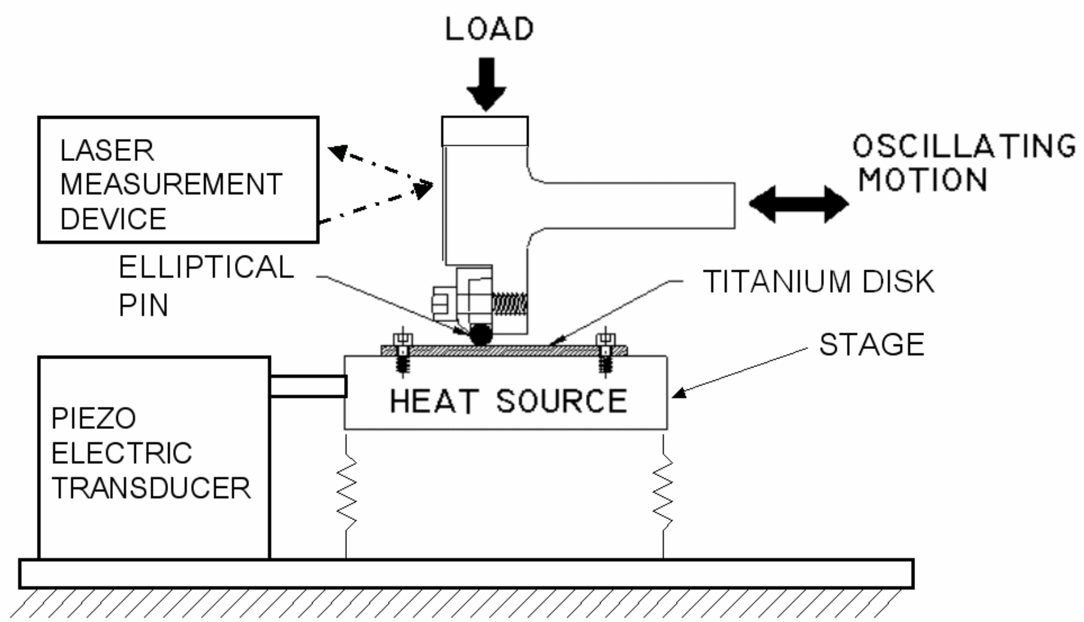

Fig. 2. Fretting wear tribometer.

Materials	Composition Weight %	Roughness Ra (μm)	Nano Hardness (GPa)	Micro Hardness (HV)	Modulus (GPa)
Copper Nickel Indium	64% Cu 35% Ni 1% In	9	2.4	138	90
Aluminum Bronze	90.3 – 87.5% Cu 9-11% Al 0.7-1.5% Fe	16	1.95	-	61
Molybdenum	Commercially pure	10	5.0	291	177
Nickel	Commercially pure	7	2.1	133	82
Titanium Substrate and Counterface	90% Ti 6% Al 4% V	0.1	4.1	284	143

Table 1. Substrate and coatings properties.

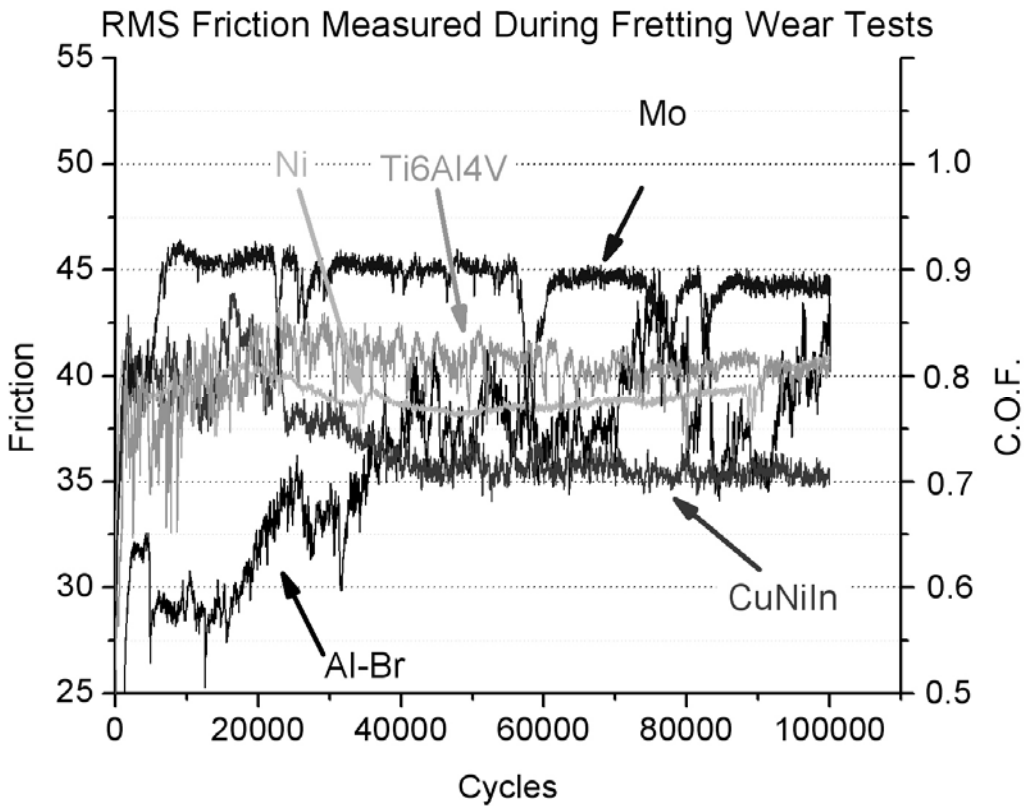

Fig. 3. RMS friction measurements for gross slip fretting at room temperature.

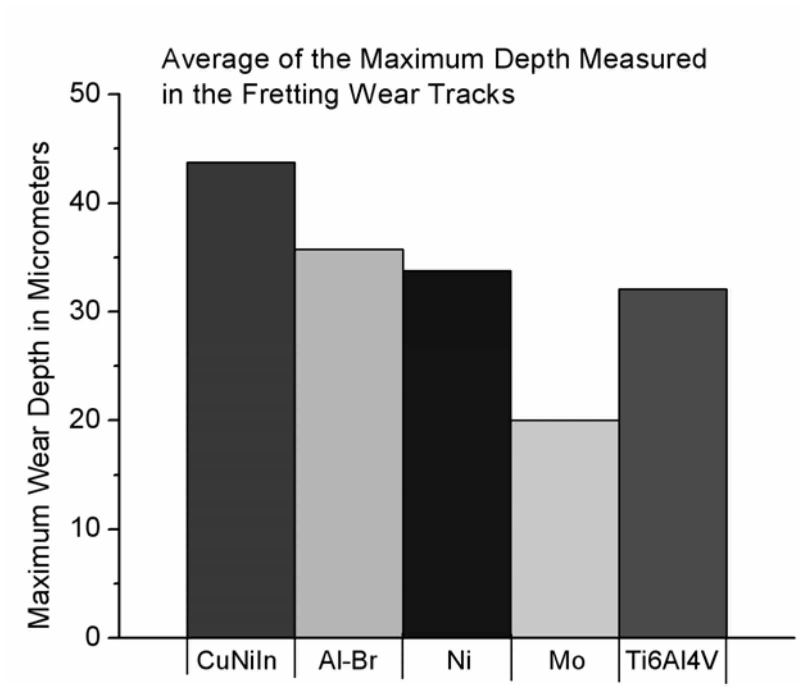

Fig. 4. Average of the maximum wear depth measured in the coating wear tracks.

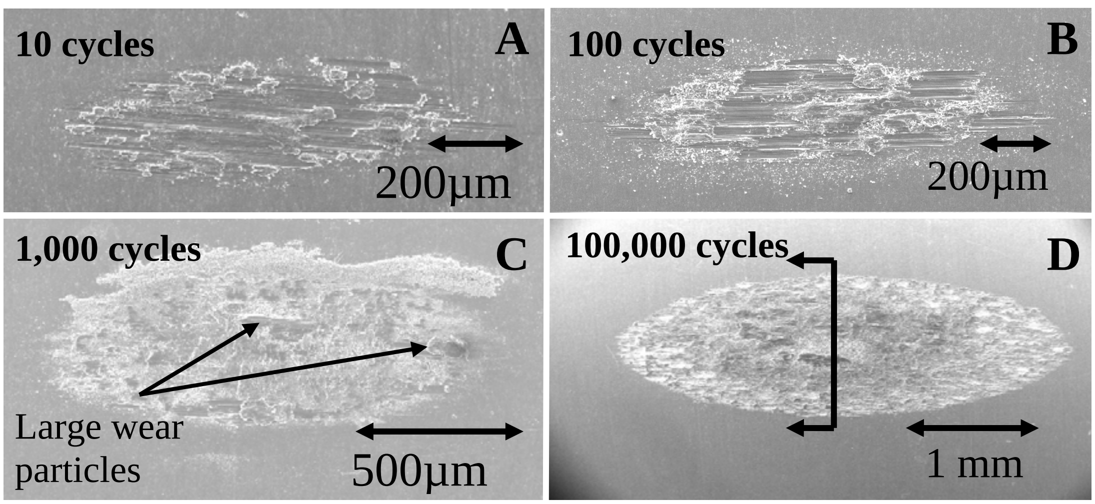

Fig. 5. SEM micrographs of the fretting wear on the surface of the ellipsoid after being worn against a Ti6Al4V uncoated disk for A) 10 cycles at 2 Hz, B) 100 cycles at 2 Hz, C) 1,000 cycles at 2 Hz, and D) 100,000 cycles at 30 Hz.

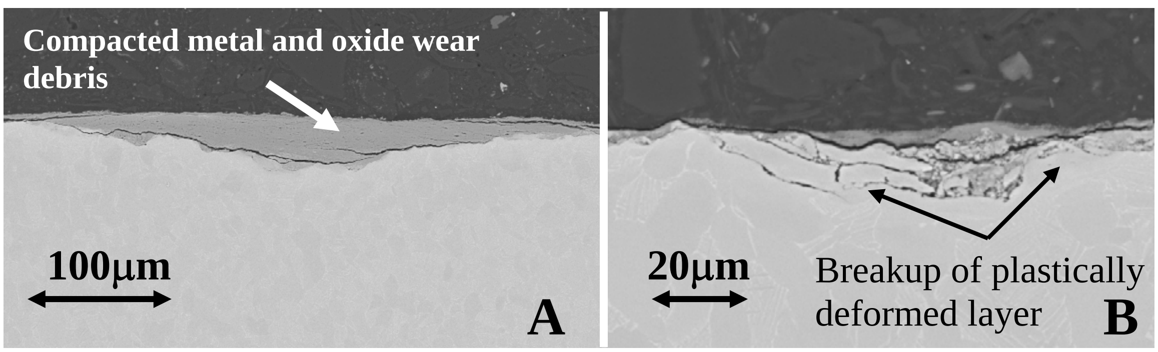

Fig. 6. Images A and B are back scatter (BSE) SEM images showing the cross-section of a Ti6Al4V ellipsoid worn against uncoated Ti6Al4V at room temperature for 100,000 cycles, at the center and edge of the wear track respectively.

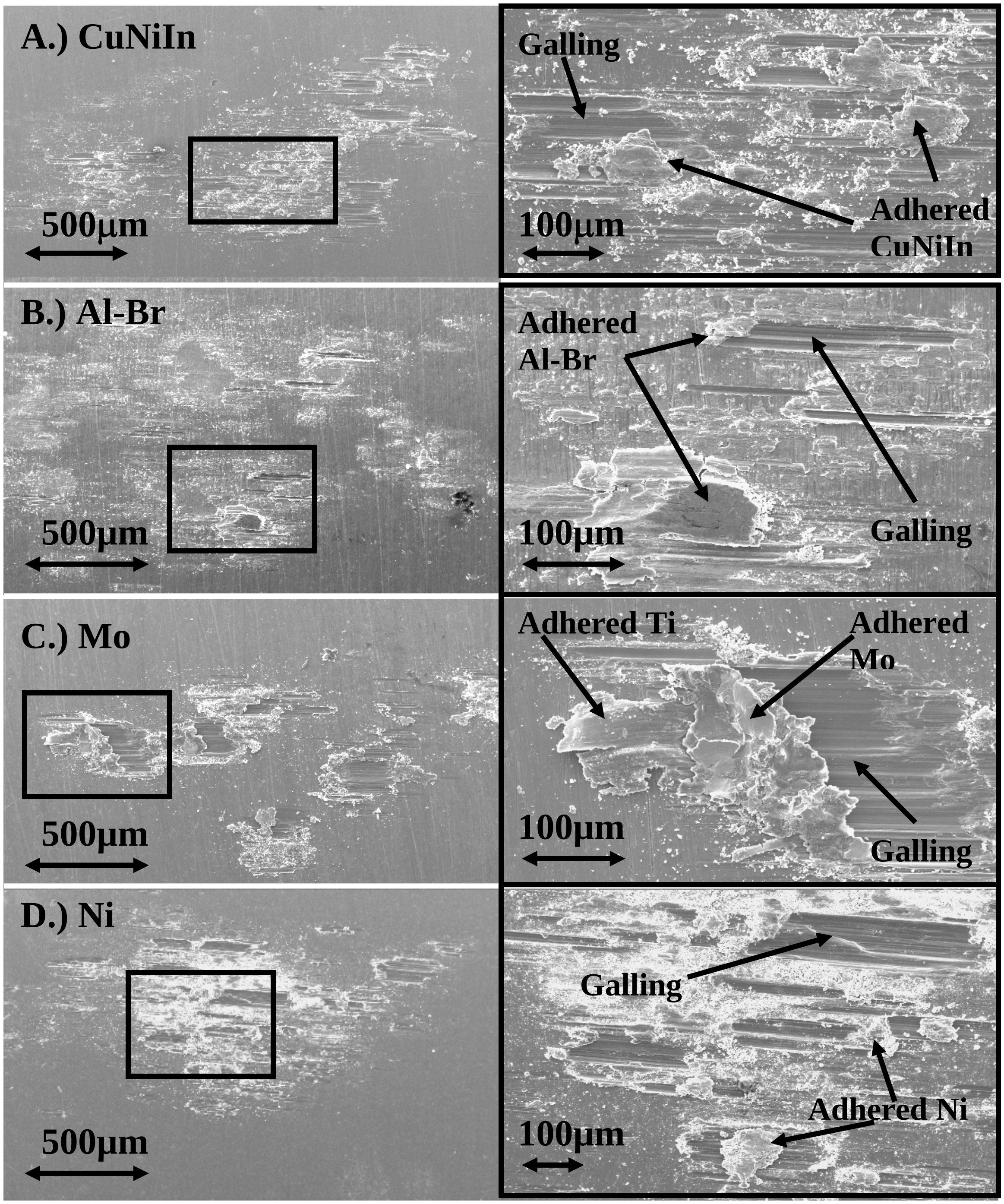

Fig. 7. SEM micrographs of the fretting wear on the surface of the Ti6Al4V ellipsoid after being worn against the test coatings for 100 cycles at 2Hz. The images outlined in black on the right are zoomed images of what is contained in the black squares on the left.

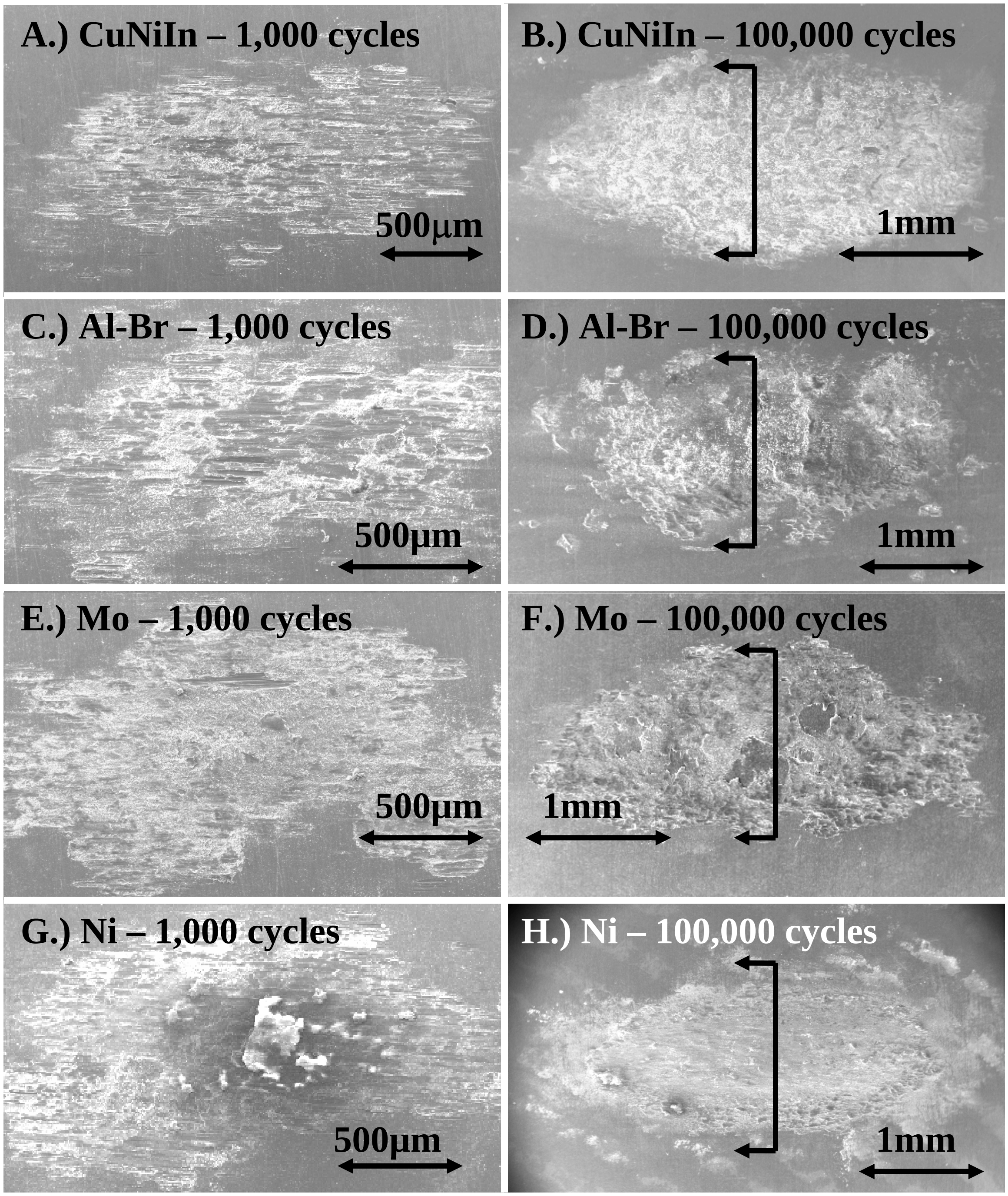

Fig. 8. SEM micrographs of the fretting wear on the surface of the Ti6Al4V ellipsoid after being worn against the test coatings at room temperature for 1,000 and 100,000 cycles respectively.

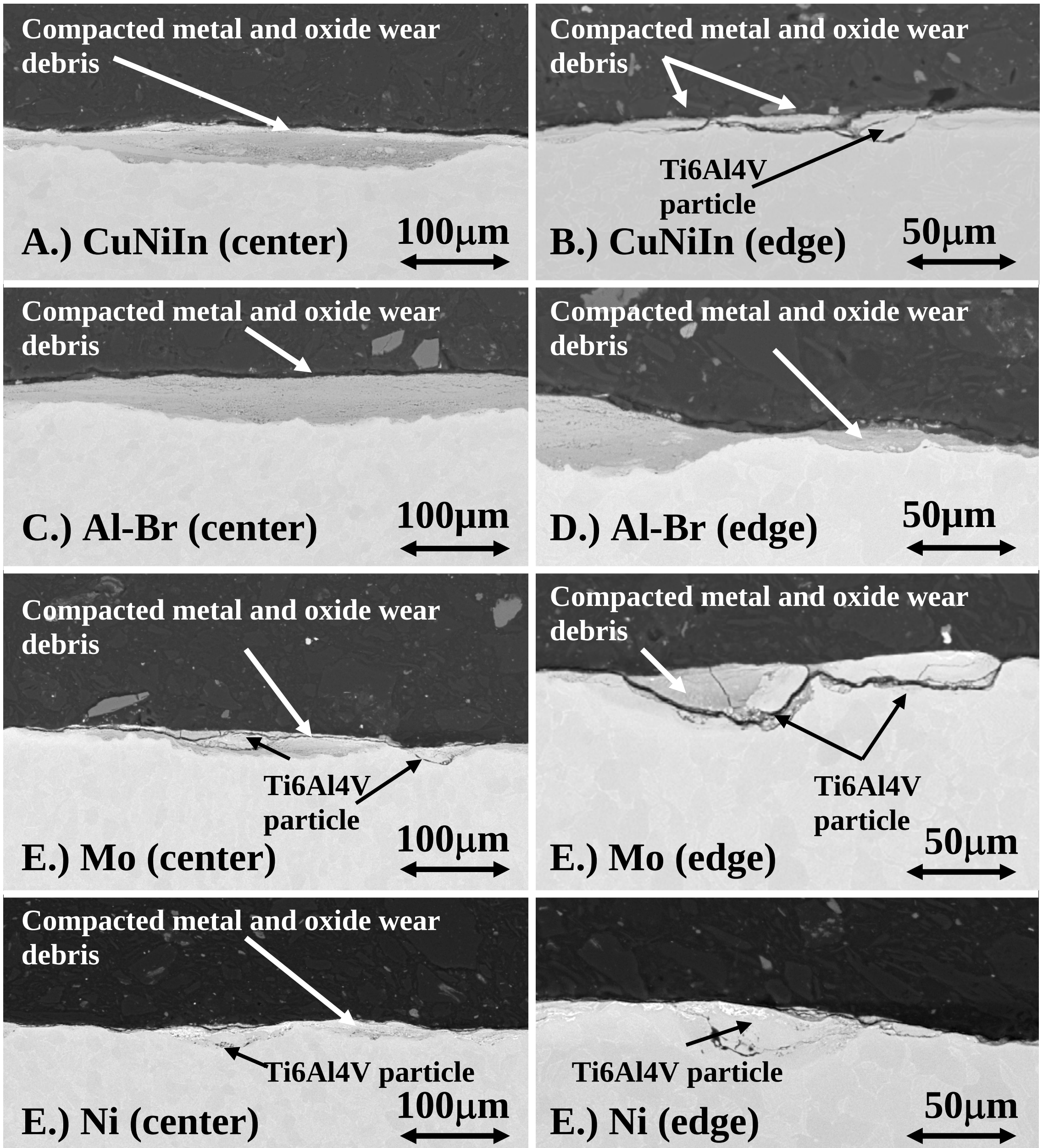

Fig. 9. Back scatter (BSE) SEM image showing the cross-section of a Ti6Al4V ellipsoid worn against the test coatings at room temperature for 100,000 cycles. Images on the left are from the center of the wear track, and images on the right are from a region near the edge of the respective wear track.

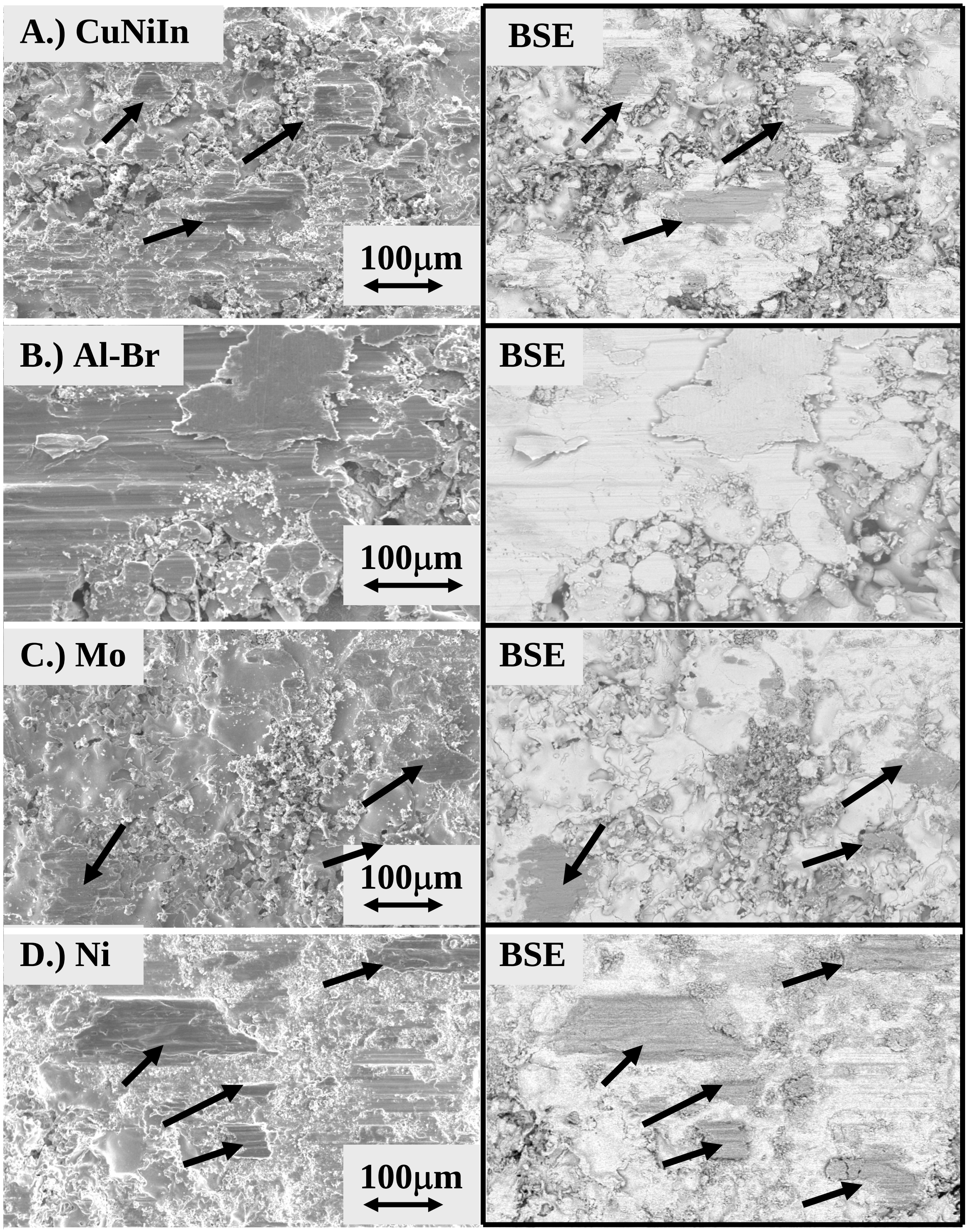

Fig. 10. SEM micrographs of the fretting wear on the surface of the test coatings after 100 cycles at 2Hz oscillation speed. On the left are secondary electron (SE) images and on the right, outlined in black, are the exact same images in using a back scatter (BSE) detector. The black arrows in all of the images point to titanium that is adhered to the coating wear surface.

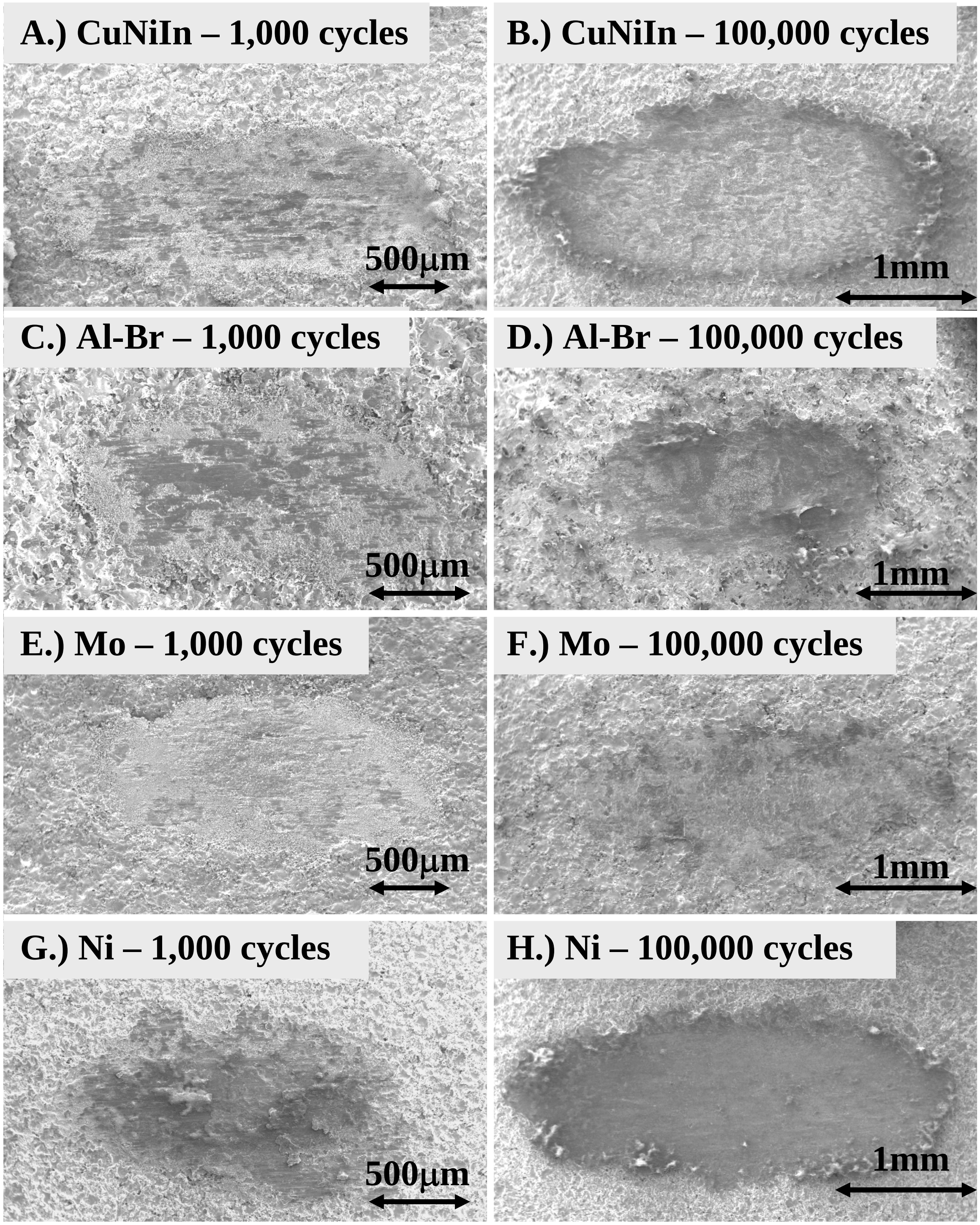

Fig. 11. SEM micrographs of the fretting wear on the surface of the test coatings after 1,000 and 100,000 cycle tests mated with Ti6Al4V.

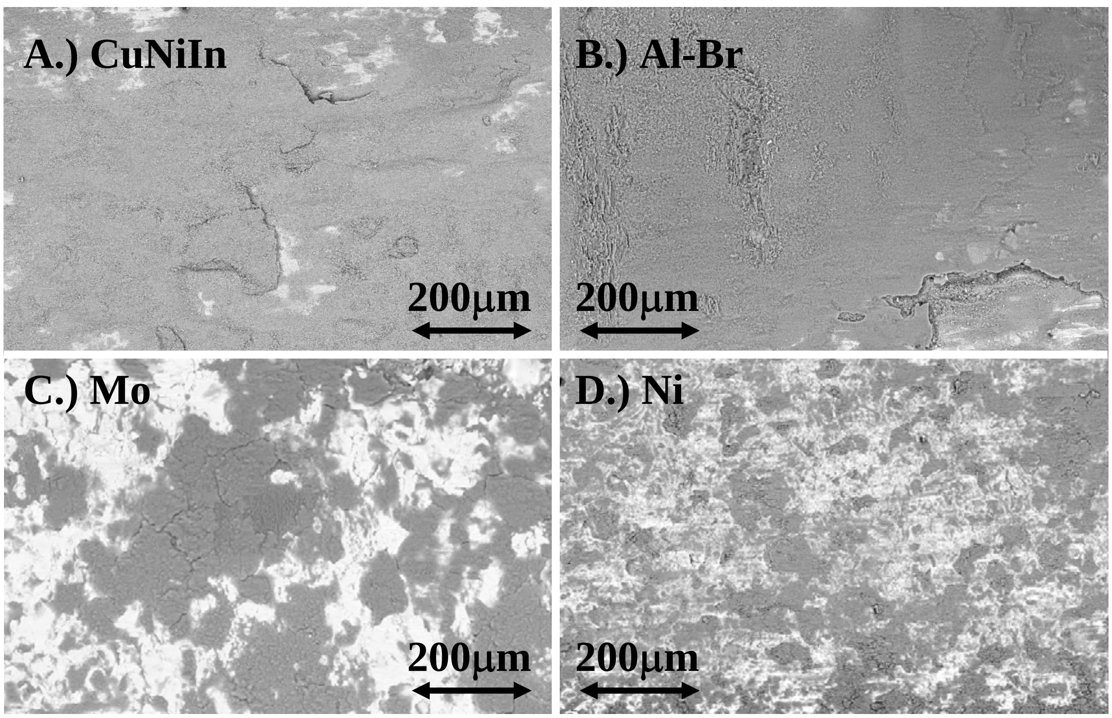

Fig. 12. Back scatter SEM micrographs of the fretting wear on the surface of the test coatings after cycle tests mated with Ti6Al4V.

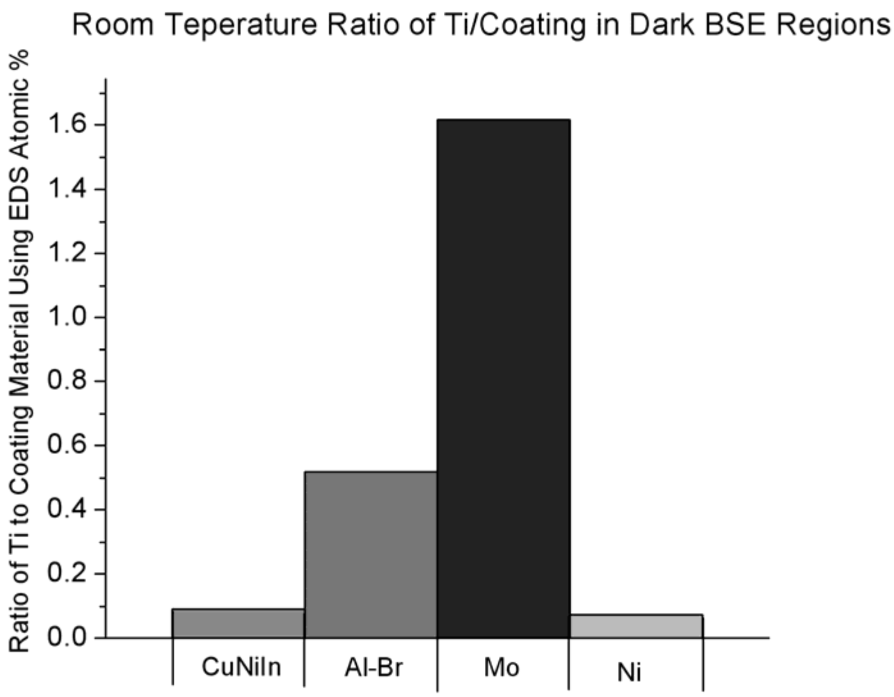

Fig. 13. Average ratio of Ti/coating in atomic % as determined from EDS scans of the dark regions shown in the BSE SEM micrographs in Fig 12.

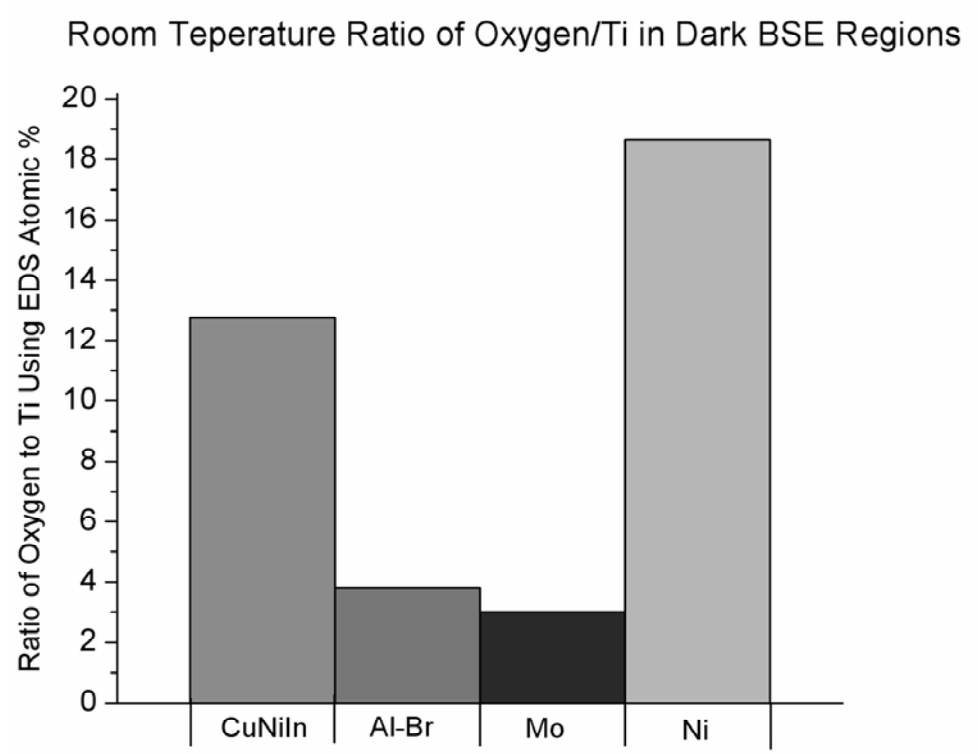

Fig. 14. Average ratio of oxygen/Ti in atomic % as determined from EDS scans of the dark regions shown in the BSE SEM micrographs in Fig 12.